Supplementary Materials I – Power spectrum rejection algorithm

We developed an algorithm to automatically reject power spectra without a sufficiently clear peak. There were a few instances in which a to-be-included power spectrum was rejected. This is not a major problem for our analyses, since the total number of rejected power spectra was rather small (50 out of 768, or ~6.5%, across 8 participants). There was no clear difference between the left (23) and right (27) hemispheres in terms of rejected power spectra. As expected, more power spectra were rejected for task data (41) as compared to rest data (9), since those data are generally noisier. Overall distributions of IAF values were similar before and after rejecting power spectra (see Figure S1).

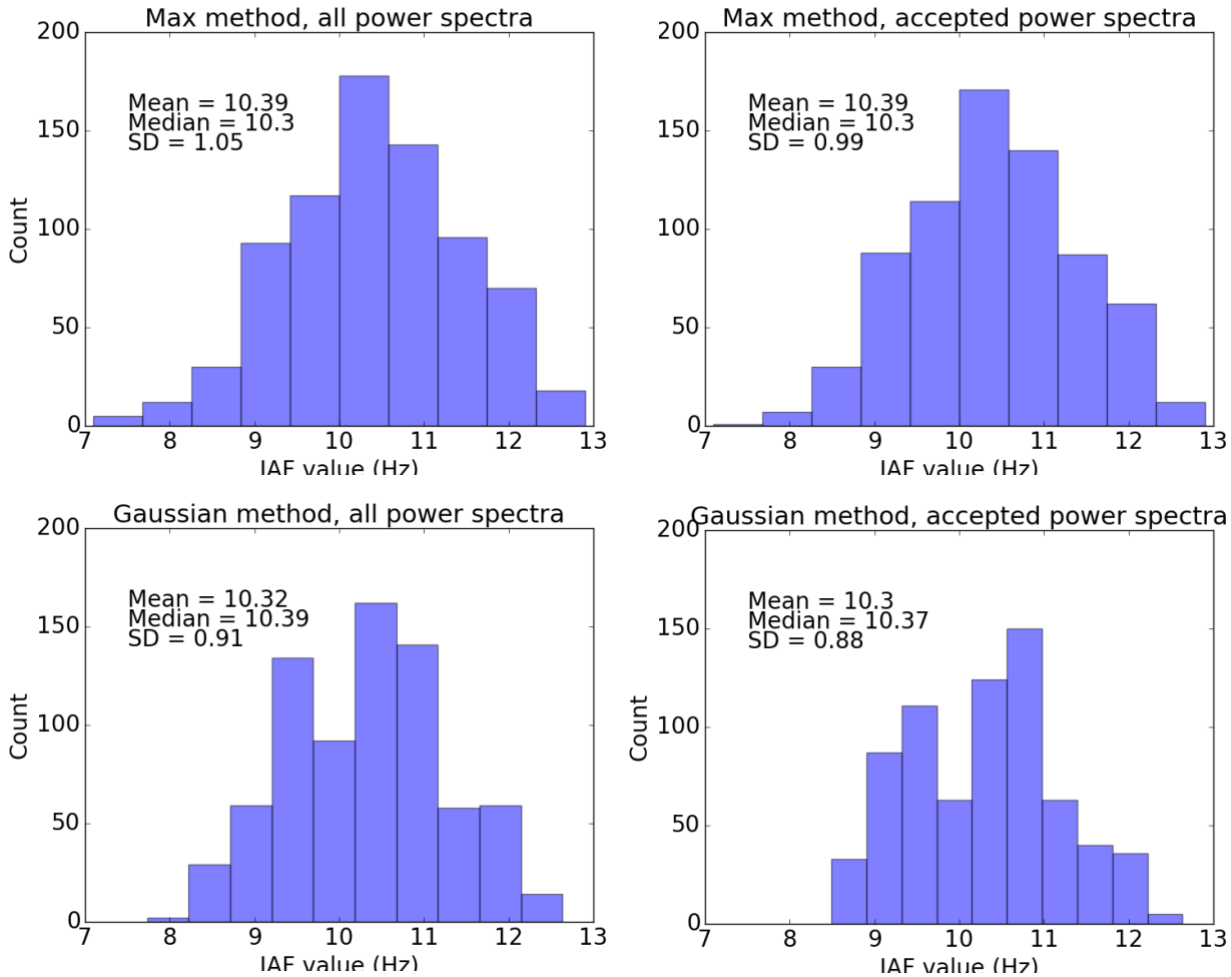

Figure S1. Distributions and descriptive statistics of IAF values as estimated by the 'maximum' method (upper row) and 'Gaussian fit' method (lower row), before (left column) and after (right column) exclusion of power spectra without a clear peak.

For the ‘Gaussian fit’ method, test-retest reliability was similarly high before and after exclusion of power spectra without a clear peak (compare Figure 4 and Figure S2, right panels). For the ‘maximum’ method, reliability increased after rejecting power spectra without a clear peak (compare Figure 4 and Figure S2, left panels).

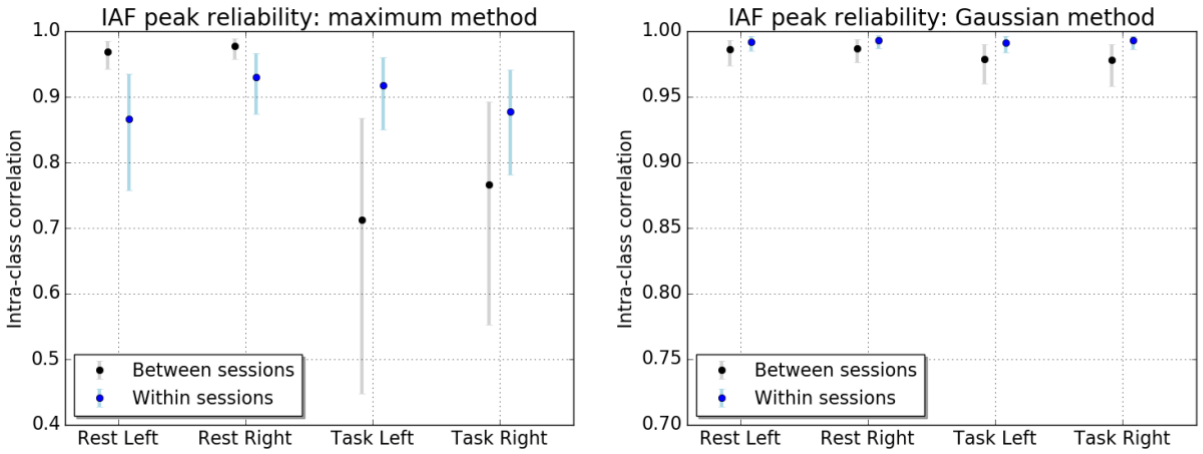

Figure S2. Test-retest reliability for IAF values as calculated with the maximum method (left panel) and the Gaussian method (right panel), before excluding power spectra. Dots indicate intra-class correlation coefficients (ICC) and surrounding lines indicate 95% confidence intervals. Between-session reliability was calculated by comparing the initial measurement of the four separate sessions (in grey). Within-session reliability was calculated by comparing the five time points of the extended session (in blue). ICC values were calculated separately per cognitive state (rest versus task) and hemisphere (left versus right).

Figure S3 provides additional examples of accepted and rejected power spectra, along with IAF results obtained with the ‘maximum’ and ‘Gaussian fit’ methods (for accepted power spectra).

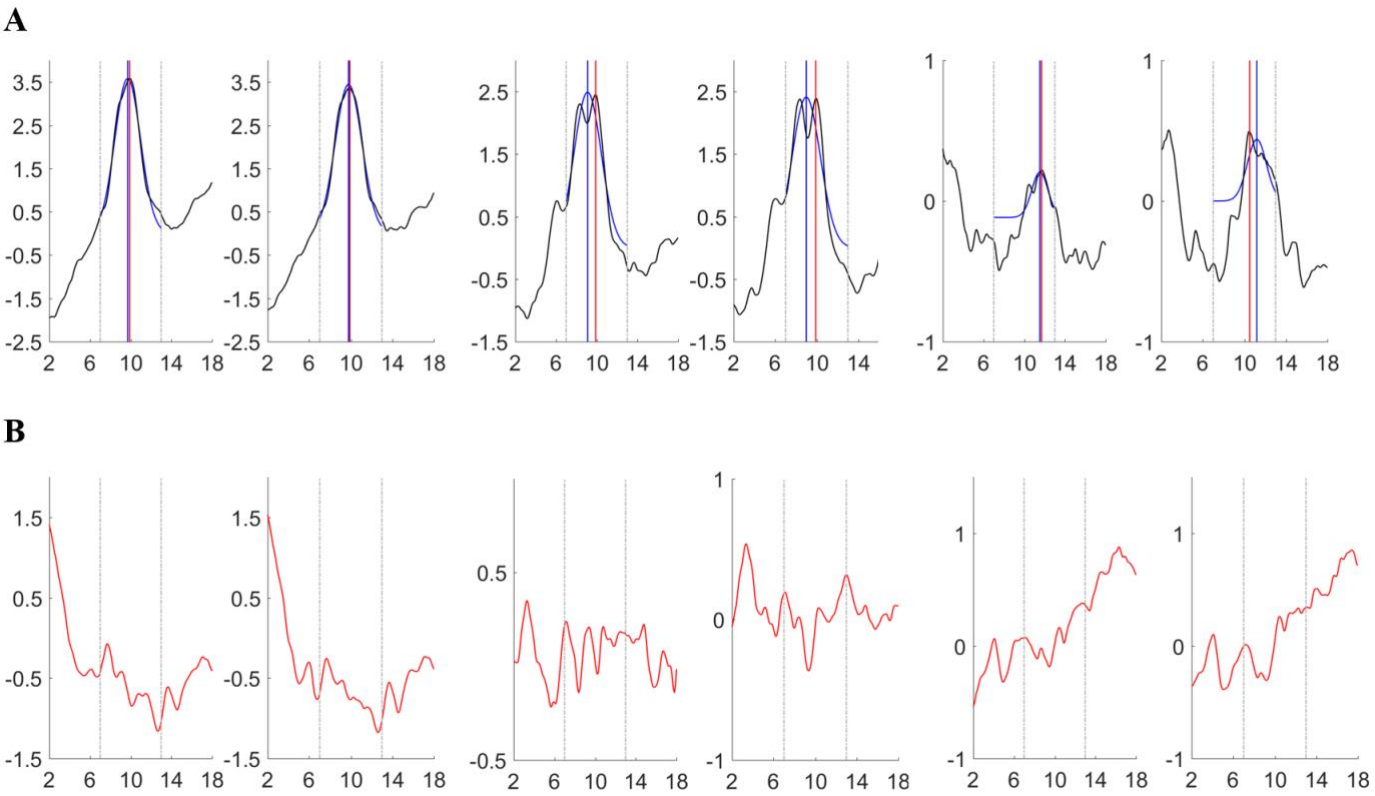

Figure S3. Power spectrum rejection, 'maximum' method, and 'Gaussian fit' method examples. **A) Representative examples of accepted power spectra**. Black lines indicate 1/f-removed and spectrally smoothed power spectra that were accepted by our power spectrum rejection algorithm. Grey vertical lines indicate the boundaries of the 7 – 13 Hertz alpha band. Red vertical lines show IAF values as obtained with the 'maximum' method. Blue vertical lines show IAF values as obtained with the Gaussian method. Blue curves show the fitted Gaussian curve. **B) Representative examples of rejected power spectra.** X-axes show frequency in Hertz, y-axes show log-transformed alpha power (uV^2).

Supplementary Materials II – Single-subject data and linear mixed model results

To quantitatively assess whether IAF estimates differed across time points, cognitive states and hemispheres, we performed two linear mixed-model analyses with a compound symmetry covariance structure, for each of the three dependent variables (IAF values as obtained by the 'maximum' method, IAF values as obtained by the 'Gaussian fit' method, and IAF width). IAF width results are reported in Supplementary Materials III. In one linear mixed model, the factor 'time' included the four initial measurements of the different sessions (between-sessions comparison). In the other linear mixed model, the factor 'time' included the five time points of the extended session (within-session comparison). Other included factors were 'cognitive state' (rest versus task) and hemisphere (left versus right, or: electrode PO3 versus PO3). Follow-up simple effects analyses were performed where necessary.

'Maximum' method

Single-subject IAF values as determined by the 'maximum' method are shown in Figure S4. The between-sessions mixed model showed a significant main effect of 'cognitive state' ($F(1, 311.31) = 20.42$, $p < 0.001$). IAF values were higher during task as compared to rest ($M = 10.52$ versus $M = 10.31$, $SE = 0.047$). Furthermore, there was a significant main effect of 'session' ($F(3, 311.06) = 2.91$, $p = 0.035$). IAF values were higher in session 3 compared to session 2 ($M = 10.52$ versus $M = 10.33$, $SE = 0.067$, $p = 0.005$ two-sided uncorrected), and higher in session 3 compared to session 4 ($M = 10.52$ versus $M = 10.38$, $SE = 0.067$, $p = 0.038$ two-sided uncorrected). The within-session mixed model showed a significant main effect of 'cognitive state' ($F(1, 406.33) = 8.29$, $p = 0.004$), with IAF values being higher during task as compared to rest ($M = 10.48$ versus $M = 10.35$, $SE = 0.043$). Note that, although statistically significant, these differences are so small (i.e., < 0.20 Hertz), that they are negligible for our purposes.

'Gaussian fit' method

Single-subject IAF values as obtained by the 'Gaussian fit' method are shown in Figure S5. The between-sessions linear mixed model analysis showed a significant effect of 'cognitive state' ($F(1, 311.06) = 6.12$, $p = 0.014$). IAF values were higher during task as compared to rest ($M = 10.33$ versus $M = 10.28$, $SE = 0.021$). The main effect of 'session' was significant as well ($F(3, 311.00) = 9.15$, $p < 0.001$). IAF values were significantly higher in session 3 ($M = 10.36$) compared to session 1 ($M = 10.28$, $SE = 0.19$, $p = 0.007$ two-tailed uncorrected) and session 2 ($M = 10.22$, $SE = 0.19$, $p < 0.001$ two-tailed uncorrected). IAF values were also higher in

session 4 (M = 10.36) compared to session 1 (M = 10.28, p = 0.007 two-tailed uncorrected) and session 2 (M = 10.23, p < 0.001 two-tailed uncorrected). The within-session mixed model showed a significant main effect of 'cognitive state' (F(1, 406.06) = 19.81, p < 0.001), a significant main effect of 'time' (F(4, 406.00) = 3.48, p = 0.008), and a significant 'time' x 'cognitive state' interaction (F(4, 406.00) = 3.15, p = 0.014). However, follow-up simple effects analyses did not show any consistent pattern of IAF over time, and differences were again of negligible magnitude.

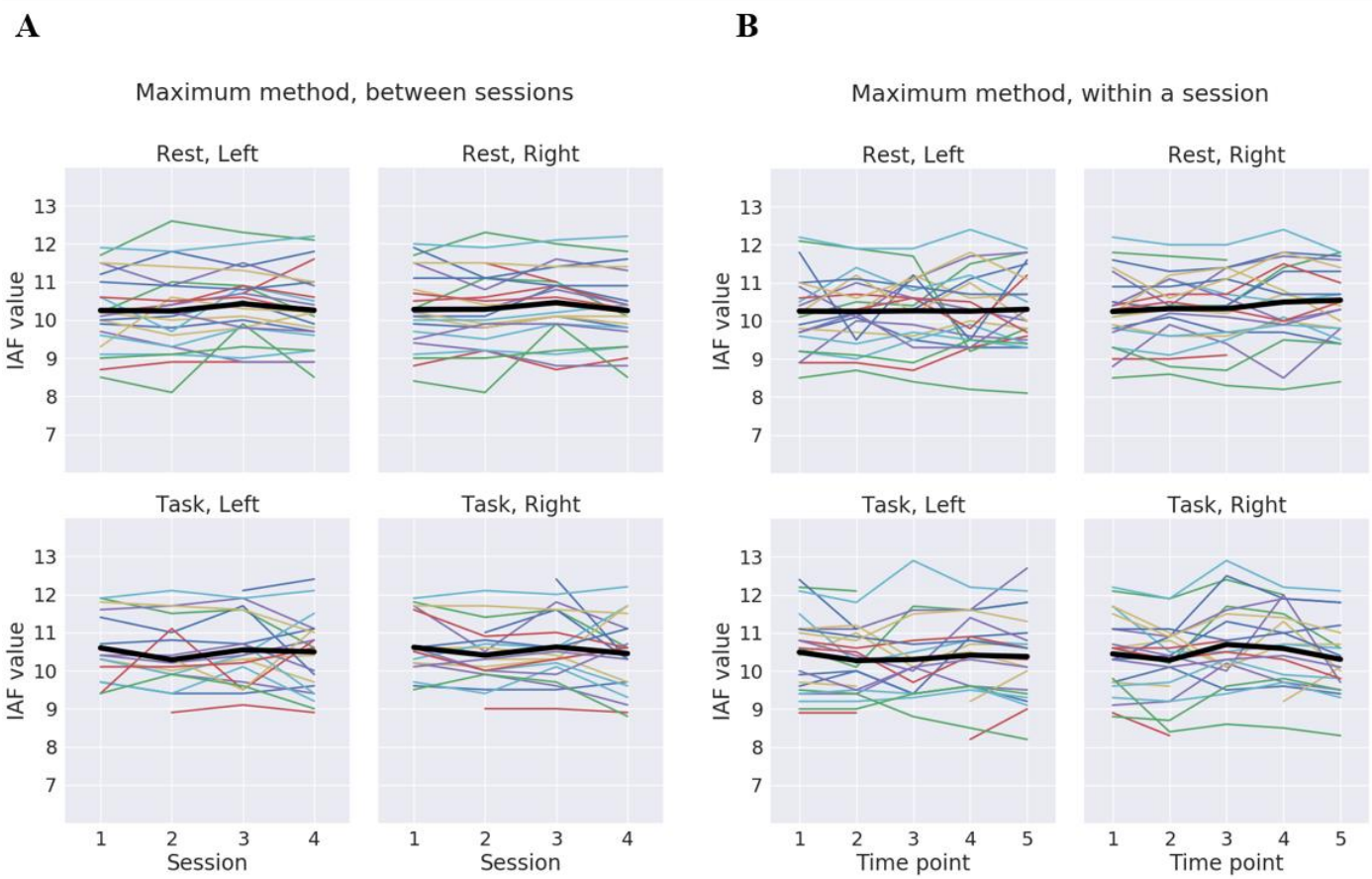

Figure S4. IAF values as estimated by the 'maximum' method. **A) Repeated IAF measurements between sessions.** IAF values are visualized separately per cognitive state and hemisphere (four sub-plots), for every initial measurement of the four sessions (x-axes). Note that sessions were counterbalanced across individuals and thus session number does not represent session order. Each colored line represents data from a single subject. Black lines indicate between-subject averages. **B) Repeated IAF measurements within a session.** Single subject data as in A), but for the five time points within the extended session.

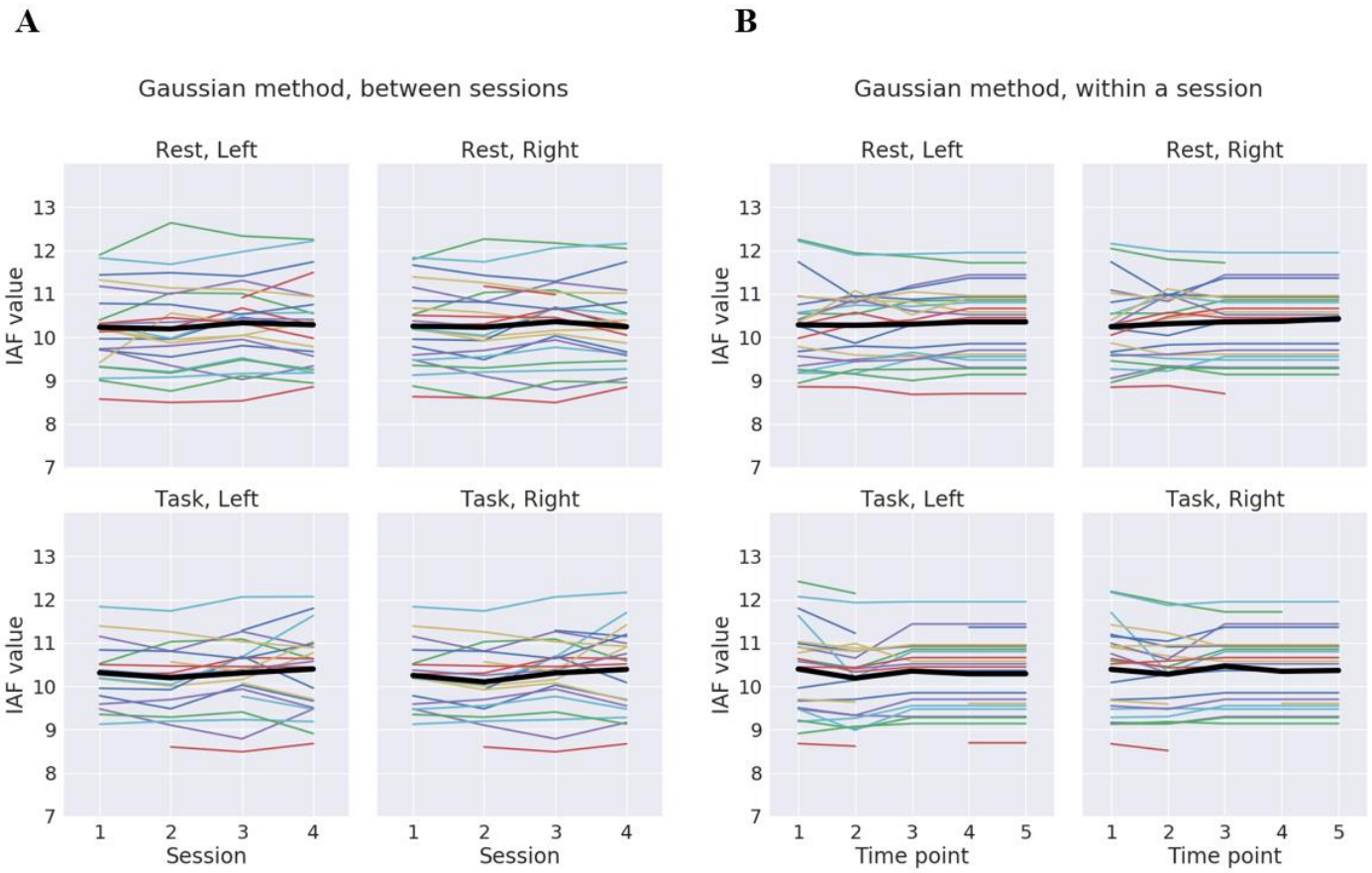

Figure S5. IAF values as estimated by the 'Gaussian fit' method. **A) Repeated IAF measurements between sessions.** IAF values are visualized separately per cognitive state and hemisphere (four sub-plots), for every initial measurement of the four sessions (x-axes). Note that sessions were counterbalanced across individuals and thus session number does not represent session order. Each colored line represents data from a single subject. Black lines indicate between-subject averages. **B) Repeated IAF measurements within a session.** Single subject data as in A), but for the five time points within the extended session.

Supplementary Materials III: IAF peak width results

To the best of our knowledge, the IAF peak width has not yet been used for individualizing rhythmic stimulation protocols. This could potentially be an interesting direction for future research, if IAF peak width shows variability between participants, is a stable individual trait just like IAF peak center, and if it can be estimated with sufficient reliability. For instance, we have recently administered individually calibrated broadband electrical brain stimulation, directly based on the IAF peak frequency as well as peak width (Janssens et al., in preparation). And as brain stimulation advances, it seems plausible that stimulation protocols will be increasingly tailored to a multitude of relevant neuroimaging markers.

How consistent are repeated IAF width estimations?

IAF peak widths were generally stable across sessions and within a session (see Figure S6), with occasional individual measurements with a seemingly incorrect result. Average IAF peak width was approximately 1.6 Hertz and did not significantly differ between cognitive states, hemispheres, or time points / sessions (all p's > 0.10). As expected, within-subject standard deviations were lower than between-subject standard deviations (see Supplementary Table 1).

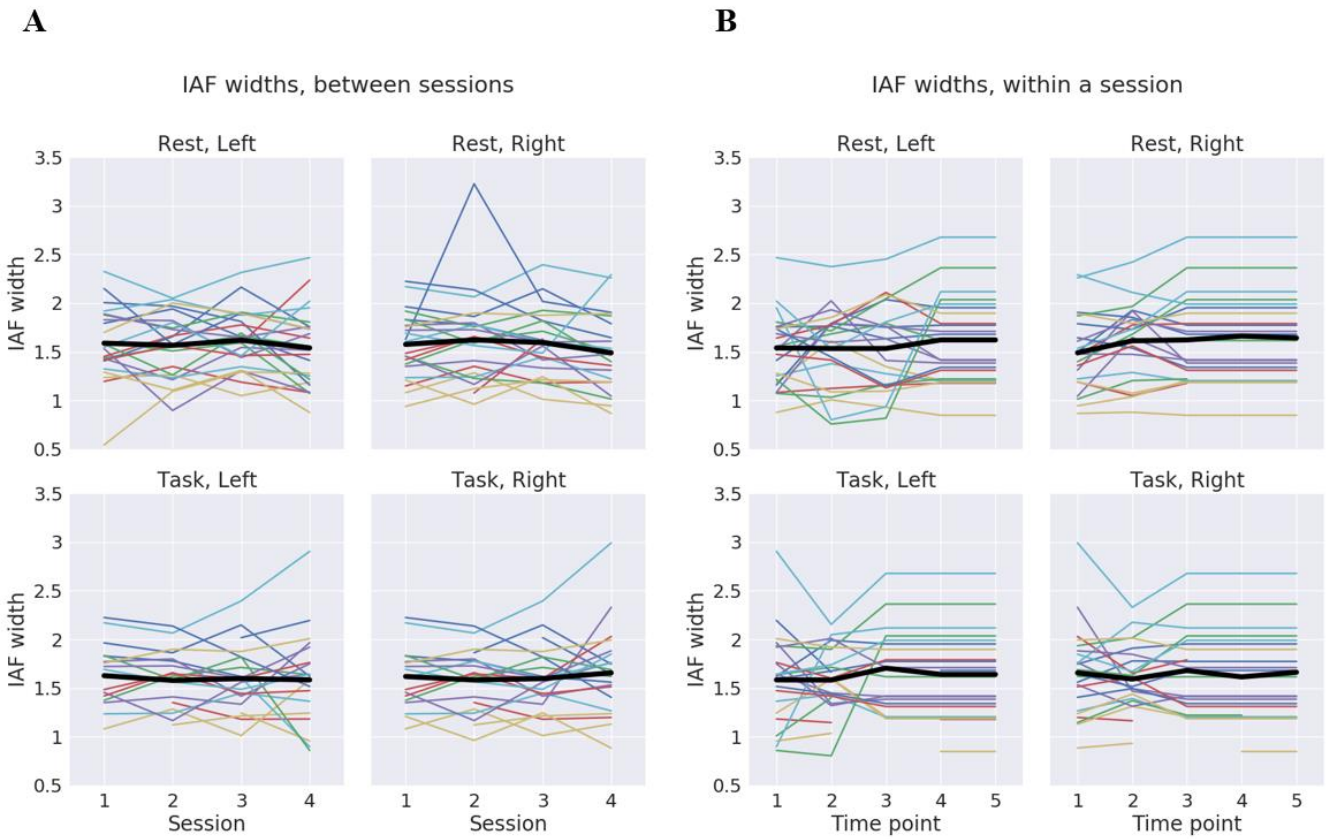

Figure S6. IAF peak widths. **A) Repeated IAF width estimations between sessions**. Peak widths are visualized for each cognitive state and hemisphere (four sub-plots), for every initial measurement of the four sessions (x-axes). Note that sessions were counterbalanced across participants and thus session number does not correspond to session order. Every colored line represents data from a single participant. Black lines show between-subject averages. **B) Repeated IAF width estimations within a session**. Same as in A), but for the five time points of the extended session.

Supplementary Table 1. Descriptive statistics for the IAF widths. Mean, minimum, maximum, and standard deviations of IAF widths are shown per cognitive state and hemisphere. 'SDwp_ws' refers to standard deviations within-participants, within-session. 'SDwp_bs' refers to standard deviations within-participants, between-sessions. 'SD_bp' refers to standard deviations between participants.

	Mean	Min	Max	SDwp_ws	SDwp_bs	SD_bp
Rest, Left	1.58	0.55	2.68	0.20	0.19	0.35
Rest, Right	1.59	0.85	3.22	0.13	0.18	0.38
Task, Left	1.61	0.81	2.90	0.19	0.20	0.35
Task, Right	1.63	0.85	2.99	0.12	0.18	0.35

ICC values were significantly larger than 0.75 for both cognitive states and hemispheres (p's < 0.05, see Figure S7), indicating that IAF width can be estimated with good test-retest reliability. Furthermore, deviation distributions generally showed low bias and low variability within- and between sessions (see Figure S8).

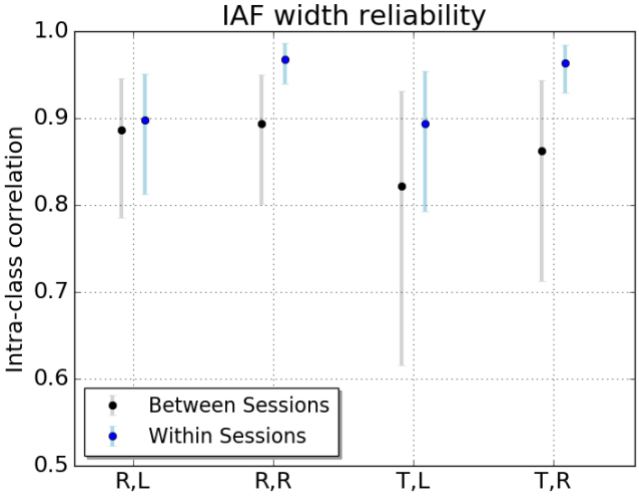

Figure S7. Reliability of IAF peak widths. Intra-class correlation coefficients (dots) are plotted with 95% confidence intervals (lines) per cognitive state (R = rest, T = task) and hemisphere (L = left, R = right).

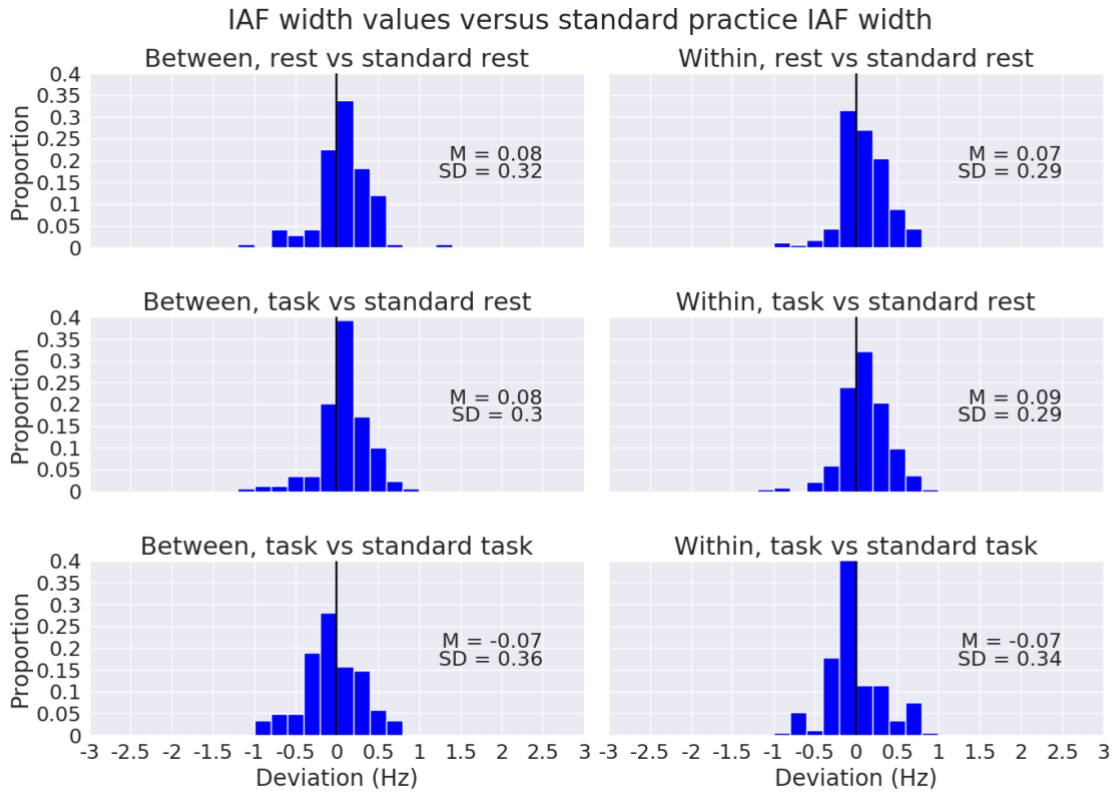

Figure S8. Deviations between repeated IAF width estimations and 'standard practice' IAF width. The upper row compares repeated rest IAF widths for all subjects and both hemispheres to the standard practice rest IAF width. For each subject, the standard practice rest IAF width was calculated by averaging the IAF widths from the left and right hemisphere, of the initial rest measurement of the extended session. The middle row compares repeated task IAF widths for all subjects and both hemispheres to the standard practice rest IAF width. The lowest row compares repeated task IAF widths for all subjects and both hemispheres to the standard practice task IAF width. Per subject, the standard practice task IAF width was calculated by averaging the IAF widths from the left and right hemisphere, of the initial measurement task data of the extended session. Between-session comparisons (left column) include data from the initial measurements of the four sessions; within-session comparisons (right column) include data from the five time points in the extended session. M = median, SD = standard deviation.

Conclusion

In sum, it appears that IAF peak width, as IAF values, can be reliably assessed as individual markers capturing a different aspect of the frequency spectrum. Results and conclusions were largely in line with those presented for the IAF values.